Progress In Electromagnetics Research C, Vol. 32, 53–63, 2012

COMPACT TRI-BAND MONOPOLE ANTENNA WITH A PARASITIC E-SHAPED STRIP FOR WLAN/WIMAX APPLICATIONS

P.-L. Shu and Q. Y. Feng*

School of Information Science and Technology, Southwest Jiaotong University, Chengdu, Sichuan 610031, China

Abstract—A compact coplanar waveguide (CPW)-fed printed monopole antenna comprising of two symmetrical C-shaped radiating elements, a parasitic E-shaped strip, and a truncated CPW ground for WLAN/WiMAX applications is proposed. By embedding a parasitic E-shaped strip inside the two symmetrical C-shaped radiating elements, four resonant frequencies and three operating bands are obtained. By etching two quarter-circles in the CPW ground, impedance matching condition of the third operating band is significantly improved. A prototype of the proposed antenna has been constructed and experimentally studied. The measured results show that three distinct operating bandwidths with 10 dB return loss are about 500 MHz (2.33–2.83 GHz), 700 MHz (3.27–3.97 GHz) and 2.37 GHz (4.3–6.67 GHz), covering all the 2.4/5.2/5.8 GHz WLAN and 2.5/3.5/5.5 GHz WiMAX bands. Furthermore, the antenna has a simple planar structure and a small volume of only $31 \times 21 \times 1.6\,\mathrm{mm}^3$. Good radiation characteristics and acceptance peak realized gains are obtained over the operating bands.

1. INTRODUCTION

With the blooming of modern wireless communication technologies, a wireless communication antenna is required to cover a very wide frequency bandwidth or several frequency bands and is expected to be small in size. For short- and long-range applications, many antennas [1–4] have been designed for the wireless local area network (WLAN) application in the 2.4 GHz (2.4–2.484 GHz)/5.2 GHz (5.15–5.35 GHz)/5.8 GHz (5.725–5.825 GHz) operating bands and the

Received 29 May 2012, Accepted 9 August 2012, Scheduled 13 August 2012
* Corresponding author: Quan Yuan Feng (fengquanyuan@163.com).

worldwide interoperability for microwave access (WiMAX) application in the 2.5 GHz (2.5–2.69 GHz)/3.5 GHz (3.3–3.8 GHz)/5.5 GHz (5.25–5.85 GHz) operating bands. Because of the advantages of low cost, easy integration, easy fabrication and omni-directional radiation pattern, the printed monopole antenna have been drawing much attention and many shapes have been reported, such as G shape [5], L shape [6], E shape [7], and C shape [8], etc.. In [9–14], dual- or tri-band antennas have been achieved, but they cannot cover all the WLAN/WiMAX bands. An effective way to obtain wideband or additional resonant frequency is to add parasitic element just like in [15–18]. But they also have the drawbacks of large in size or complicated in structures with double metallic layer.

In this paper, a compact printed monopole antenna for WLAN/WiMAX applications is proposed. Because of the outstanding features of single metallic layer, broad bandwidth, smaller mutual coupling between adjacent lines and easier integration with system circuits, coplanar waveguide (CPW)-fed structure has been widely used [19–21] and thus incorporated in the design of the proposed antenna. By embedding a parasitic E-shaped strip inside the two symmetrical C-shaped radiating elements and etching two quarter-circles in the CPW ground, the proposed antenna can generate four resonant frequencies at 2.6/3.6/4.7/6.4 GHz which are formed into three wide bands (2.33–2.83 GHz, 3.27–3.97 GHz and 4.30–6.67 GHz) to cover all the WLAN and WiMAX operating bands. The proposed antenna also shows good radiation characteristics with small cross-polarization level and acceptance peak realized gains over the operating bands.

2. ANTENNA DESIGN

Figure 1(a) illustrates the geometry of the proposed tri-band printed monopole antenna for WLAN/WiMAX application. The antenna consists of two C-shaped radiating elements that are symmetrically connected to a CPW feed line, a parasitic E-shaped strip, and a truncated CPW ground. The 50 Ω CPW feeding mechanism has a signal strip width of $W_f = 2.5$ mm and a gap distance of $S = 0.3$ mm between the signal strip and the truncated CPW ground. In order to achieve more resonant frequencies and wideband, the parasitic E-shaped strip is embedded inside the two C-shaped radiating elements without increasing the size of the antenna. Furthermore, two quarter-circles with radius $R_0 = 2$ mm are etched from the CPW ground, which play an important role in improving the impedance match of the proposed antenna in 5.5 GHz band.

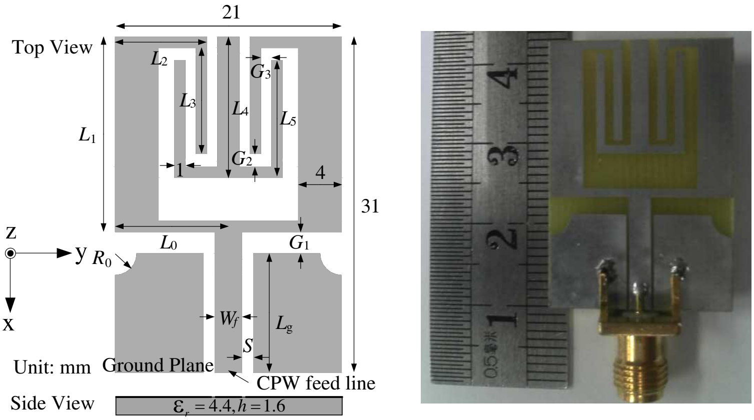

(a) (b)

Figure 1. (a) Geometry of the proposed CPW-fed tri-band antenna, and (b) photograph of the fabricated antenna.

The proposed antenna is printed on a low-cost FR4 substrate with thickness (h) of 1.6 mm, relative permittivity (ε_r) of 4.4, and loss tangent of 0.02. The volume of the proposed antenna is only $31 \times 21 \times 1.6\,\text{mm}^3$. As both the radiating elements and the CPW feeding mechanism are implemented on the same plane; hence, fabrication of the proposed antenna is very easy using a single-sided metallization process.

For detailed design, Ansoft HFSS based on finite element method (FEM) has been employed to analyze and optimize the electrical properties and radiation characteristics of the antenna. Via iterative design process, the proper parameters for optimal tri-band operation of the proposed antenna are set as follows: $G_1 = 2\,\text{mm}$, $G_2 = 0.5\,\text{mm}$, $G_3 = 1\,\text{mm}$, $L_0 = 10.5\,\text{mm}$, $L_1 = 18\,\text{mm}$, $L_2 = 8.5\,\text{mm}$, $L_3 = 10.5\,\text{mm}$, $L_4 = 13\,\text{mm}$, $L_5 = 11.5\,\text{mm}$, $L_g = 11\,\text{mm}$, $R_0 = 2\,\text{mm}$. Figure 1(b) is the photograph of the fabricated antenna.

Various CPW-fed monopole antennas involved in the antenna design evolution process for tri-band operation are shown in Figure 2. Antenna 1 consists of two C-shaped radiating elements and a CPW ground without any truncation. This simple monopole antenna (Antenna 1) generates a quite wide dual-band operation resonated at 2.8/4.7 GHz, ranging from 2.19 to 3.14 GHz and 3.87 to 5.73 GHz. It covers the 2.4/5.2 GHz WLAN and 2.5 GHz WiMAX application. With an additional parasitic E-shaped strip embedded in Antenna 1, another two resonant frequencies are excited at 3.7/6.4 GHz without

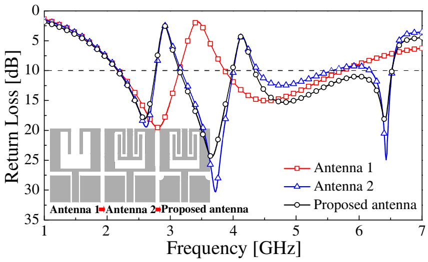

Figure 2. Design evolution of the proposed tri-band antenna and its corresponding simulated return loss results.

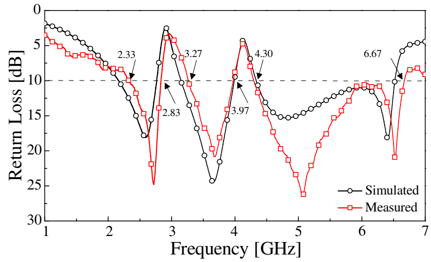

Figure 3. Measured and simulated return loss for the proposed antenna.

enhancing its size and three operating bands are achieved. Because of electromagnetic coupling between the two C-shaped radiating elements and the parasitic E-shaped strip, the lower resonant frequency (2.8 GHz) of Antenna 1 shifts down to 2.6 GHz but the upper resonant frequency (4.7 GHz) changes a little. It can be seen that the impedance bandwidths of Antenna 2 range from 2.19 to 2.78 GHz, 3.18 to 4 GHz and 4.4 to 6.52 GHz. But the impedance matching of the highest operating band is poor. At last, two quarter-circles are etched from the CPW ground, as the proposed antenna, impedance matching condition of the highest operating band can be significantly improved and thus three distinct wide bandwidths for all the 2.4/5.2/5.8 GHz WLAN and 2.5/3.5/5.5 GHz WiMAX applications are obtained. By utilizing these specialized design structures, the antenna can yield four resonant frequencies and three distinct operating bands to cover the required bands while maintaining compact size and simple structure.

3. EXPERIMENTAL RESULTS AND DISCUSSION

A fabricated prototype of the proposed tri-band printed monopole antenna has been experimentally studied, as depicted in Figure 1(b). The return loss was measured with Agilent E5071C ENA network analyzer. Figure 3 presents the measured and simulated return loss against frequency for the proposed antenna. From the measured results, three distinct operating bandwidths with 10 dB return loss are about 500 MHz (2.33–2.83 GHz), 700 MHz (3.27–3.97 GHz) and 2.37 GHz (4.30–6.67 GHz), corresponding to an impedance bandwidth of 19.4, 19.3, and 43.2% with respect to the center frequency, respectively. And it is easy to cover all the required bandwidths for

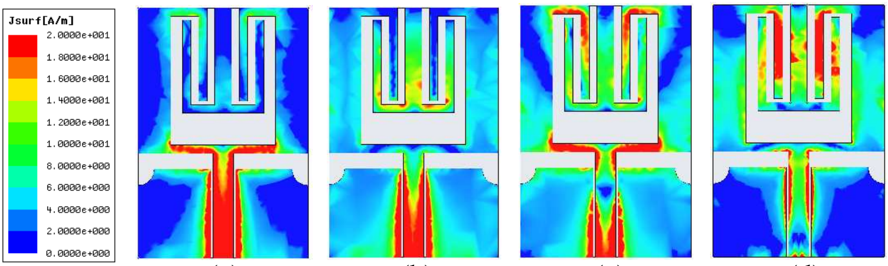

(a) (b) (c) (d)

Figure 4. Simulated surface current distributions of the proposed antenna at (a) 2.6, (b) 3.6, (c) 4.7, and (d) 6.4 GHz.

WLAN and WiMAX bands applications. Good agreement between the simulation and measurement can be observed, although the measured return loss shift slightly to higher frequency. However, the reasons attributed to the differences are believed 1) the manufacturing tolerances about the related physical parameter; 2) the uncertainty of the thickness and/or the dielectric constant of the FR4 substrate; and 3) the coupling between the SMA connector and various parts of the antenna.

In order to further demonstrate the tri-band operation mechanism, surface current distributions on the whole proposed antenna at four resonant frequencies are shown in Figure 4. It can be clearly seen that the current has different distributions along the antenna in different bands. In Figure 4(a), the surface current density launched from the CPW feeder is mainly concentrated along inner edges of the two C-shaped radiating elements with $G_1 + L_0 + L_1 + L_2 + L_3 =$ 49.5 mm current length, which corresponds to 0.44 wavelength at 2.6 GHz. It indicates that fundamental resonant mode at 2.6 GHz of the two C-shaped radiating elements is excited. At the 3.6 GHz resonant frequency, the surface current is mainly concentrated at the parasitic E-shaped strip, as depicted in Figure 4(b). The two C-shaped radiating elements work as a feeding structure at 3.6 GHz and radiation occurs mainly on the parasitic E-shaped strip. Strong surface current distributions along the top bending part of the two C-shaped radiating elements at 4.7 GHz is also seen, which demonstrates that another resonant mode of the two C-shaped radiating elements is excited. At the 6.4 GHz resonant frequency, the surface current is concentrated at the two C-shaped radiating elements and the parasitic E-shaped strip, as shown in Figure 4(d), indicating that electromagnetic coupling between the two C-shaped radiating elements and the parasitic E-shaped strip generate this resonance. With the help of the two adjacent

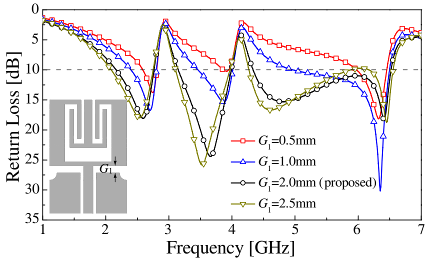

Figure 5. Simulated return loss of the proposed antenna with different G_1.

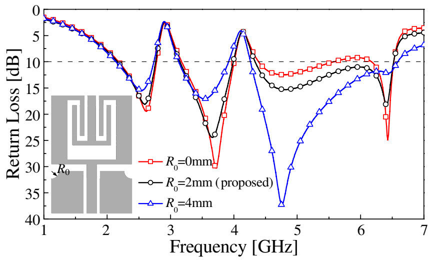

Figure 6. Simulated return loss of the proposed antenna with different R_0.

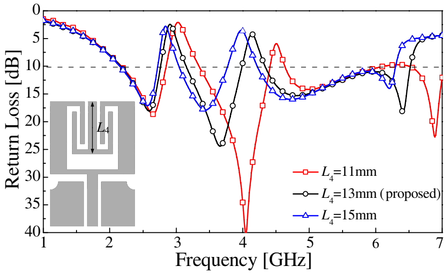

Figure 7. Simulated return loss of the proposed antenna with different L_4.

resonant frequencies at 4.7 GHz and 6.4 GHz, a very wide operating band (4.30–6.67 GHz) is achieved for 5.2/5.8 GHz WLAN and 5.5 GHz WiMAX applications.

The gap G_1 between the radiating elements and CPW ground is a critical parameter to control the impedance bandwidth, as shown in Figure 5. Clearly, as the decrease of G_1, the bandwidths of the proposed antenna tend to be narrow. Consequently, three distinct broad bandwidths have been obtained in case of $G_1 = 2$ mm. In addition, the radius of the etched two quarter-circles in the CPW ground plays an important role in impedance matching condition, as shown in Figure 6. As the radius R_0 increases, the lower two resonant frequencies are decreased a little, with the deteriorated matching in the lower two band but the improved matching in the upper band. In this case, the preferred value of R_0 is 2 mm. Effects of the parasitic E-shaped strip length L_4 on resonant frequencies are also studied, as shown in Figure 7. Varying L_4 from 11 to 15 mm with an increment of 2 mm, the second and last resonant frequencies are clearly seen to

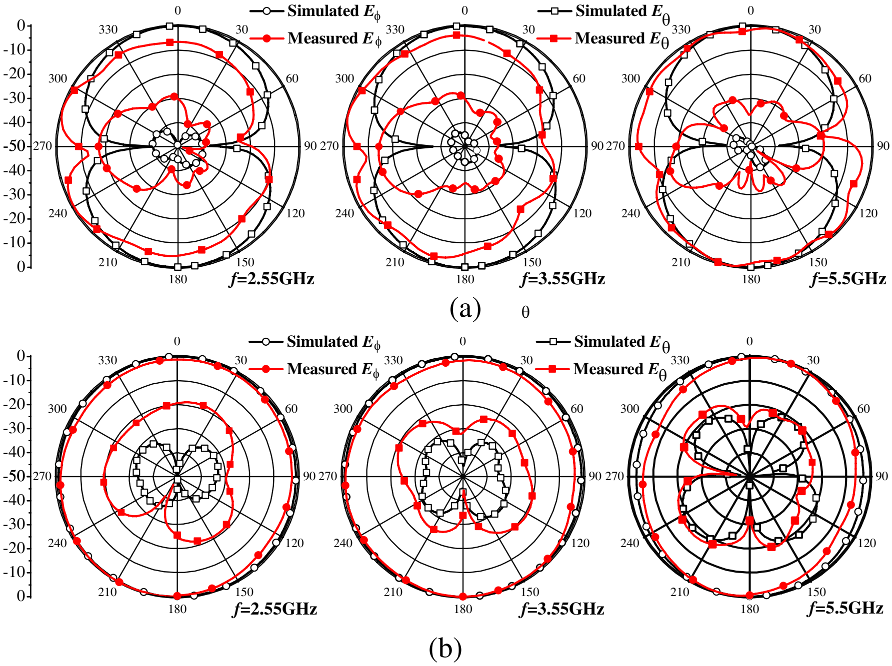

Figure 8. Measured and simulated normalized radiation patterns at 2.55, 3.55, and 5.5 GHz in (a) E-plane (x-z plane) and (b) H-plane (y-z plane).

move toward the lower frequency. However, except for some change of matching condition at the other frequencies, no significant effects in resonance condition are found. According to this, the value of 13 mm for L_4 is therefore selected for the proposed antenna to search for appropriate resonant frequencies and optimal operating bandwidths.

The radiation patterns of the proposed antenna were measured in a microwave anechoic chamber (SATIMO near-field measurement system). Figure 8 shows the measured and simulated far-field normalized radiation patterns including the vertical (E_θ) and horizontal (E_φ) polarization in the E-plane (x-z plane) and H-plane (y-z plane) of the proposed antenna. The obtained radiation patterns have bidirectional radiations in E-plane and nearly omnidirectional radiations in H-plane. A good agreement between the measured and simulated radiation patterns are observed except for the horizontal (E_φ) polarization in E-plane. This is mainly due to the spurious reflections from SMA connector and RF cable that are not incorporated in the simulation. In general, stable radiation patterns within the

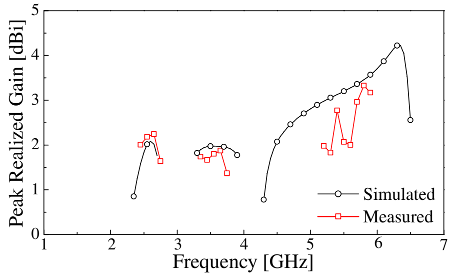

Figure 9. Measured and simulated peak realized gains.

Table 1. Comparison results of the proposed and reference antennas.

Reference	Proposed	[3]	[15]	[22]	[23]
Size (mm^3)	31×21 ×1.6	38×25×1.59	38× 36×1.6	32×28 ×1	50×50 ×1.6
Operating bands (GHz)	2.33~2.83 3.27~3.97 4.30~6.67	2.40–2.70 3.10–4.15 4.93–5.89	2.29–2.66 3.42–6.39	2.34–2.82 3.16–4.06 4.69–5.37	2.38~2.99 4.96~6.41
Layer	Single	Double	Single	Single	Single

operating bands are achieved and the cross-polarization level is very small in the H-plane. Having taken the impedance mismatch into account, the measured and simulated peak realized gains of the proposed antenna are depicted in Figure 9. The measured average peak realized gains are about 2.02 dBi from 2.4 GHz to 2.75 GHz, 1.69 dBi from 3.3 GHz to 3.8 GHz and 2.52 dBi from 5.1 GHz to 5.9 GHz, respectively. Due to large dielectric loss of the FR4 substrate at high frequencies, the measured gains in the middle and upper band are relatively small compared with the simulated results. However, the gains of the proposed antenna still satisfy the requirement of some actual applications.

The performances of the proposed antenna are compared with those of the recently reported WLAN and/or WiMAX antennas [3, 15, 22, 23] in Table 1. Although the proposed antenna is realized with a relatively compact size, it provide competitively enhanced bandwidths covering all the 2.4/5.2/5.8 GHz WLAN and 2.5/3.5/5.5 GHz WiMAX bands. Moreover, it is easy to fabricate and low cost owing to the single layer. Because of the excellent far-field characteristics and appropriate return loss in the three operating bands, the proposed antenna is suitable for WLAN and WiMAX wireless communication systems application.

4. CONCLUSION

A compact CPW-fed tri-band printed monopole antenna has been presented. By embedding a parasitic E-shaped strip inside the two symmetrical C-shaped radiating elements and etching two quarter-circles in the ground, three distinct operating bands which can meet all the requirements for WLAN and WiMAX standard are obtained, ranging from 2.33–2.83 GHz, 3.27–3.97 GHz and 4.30–6.67 GHz, respectively. The proposed antenna has the advantages of simple structure, easy fabrication, low cost, and compact size, showing good tri-band operating bandwidth and stable radiation patterns. Consequently, the proposed antenna is expected to be a good candidate for WLAN/WiMAX wireless communication systems.

ACKNOWLEDGMENT

This work is supported by the National Natural Science Foundation of China (NSFC) under Grants 60990320, 60990323 and the National 863 Project of China under Grant 2012AA012305.

REFERENCES

1. Ren, X.-S., Y.-Z. Yin, W. Hu, and Y.-Q. Wei, "Compact tri-band rectangular ring patch antenna with asymmetrical strips for WLAN/WiMAX applications," *Journal of Electromagnetic Waves and Applications*, Vol. 24, No. 13, 1829–1838, 2010.
2. He, K., R.-X. Wang, Y.-F. Wang, and B.-H. Sun, "Compact tri-band claw-shaped monopole antenna for WLAN/WiMAX applications," *Journal of Electromagnetic Waves and Applications*, Vol. 25, Nos. 5–6, 869–877, 2011.
3. Pei, J., A. Wang, S. Gao, and W. Leng, "Miniaturized triple-band antenna with a defected ground plane for WLAN/WiMAX applications," *IEEE Antennas and Wireless Propagation Letters*, Vol. 10, 298–301, 2011.
4. Zhuo, Y., L. Yan, X. Zhao, and K. M. Huang, "A compact dual-band patch antenna for WLAN applications," *Progress In Electromagnetics Research Letters*, Vol. 26, 153–160, 2011.
5. Liu, W. C., "Optimal design of dualband CPW-fed G-shaped monopole antenna for WLAN application," *Progress In Electromagnetics Research*, Vol. 74, 21–38, 2007.
6. Zhang, T.-L., Z.-H. Yan, L. Chen, and Y. Song, "A compact dual-band CPW-fed planar monopole antenna for

WLAN applications," *Journal of Electromagnetic Waves and Applications*, Vol. 22, Nos. 14–15, 2097–2104, 2008.

7. Ali Nezhad, S. M. and H. R. Hassani, "A novel triband E-shaped printed monopole antenna for MIMO application," *IEEE Antennas and Wireless Propagation Letters*, Vol. 9, 576–579, 2010.
8. Han, Y., Y.-Z. Yin, Y.-Q. Wei, Y. Zhao, B. Li, and X.-N. Li, "A novel triple-band monopole antenna with double coupled C-shaped strips for WLAN/WiMAX applications," *Journal of Electromagnetic Waves and Applications*, Vol. 25, Nos. 8–9, 1308–1316, 2011.
9. Li, C. M., K. Wang, and C. K. Chen, "Small tri-band monopole antenna for WiMAX/WLAN applications," *Journal of Electromagnetic Waves and Applications*, Vol. 25, Nos. 8–9, 1297–1307, 2011.
10. Lu, J.-H. and Y.-H. Li, "Planar multi-band T-shaped monopole antenna with a pair of mirrored L-shaped strips for WLAN/WiMAX operation," *Progress In Electromagnetics Research C*, Vol. 21, 33–44, 2011.
11. Zhang, S.-M., F.-S. Zhang, W.-M. Li, W.-Z. Li, and H.-Y. Wu, "A multi-band monopole antenna with two different slots for WLAN and WiMAX applications," *Progress In Electromagnetics Research Letters*, Vol. 28, 173–181, 2012.
12. Tang, I.-T., C.-M. Li, and C.-H. Hung, "Octa-band LV-shape CPW-fed monopole antenna," *Journal of Electromagnetic Waves and Applications*, Vol. 25, No. 10, 1471–1480, 2011.
13. Lee, C.-T., S.-W. Su, and F.-S. Chang, "A compact, planar plate-type antenna for 2.4/5.2/5.8-GHz tri-band WLAN operation," *Progress In Electromagnetics Research Letters*, Vol. 26, 125–134, 2011.
14. Panda, J. R. and R. S. Kshetrimayum, "A printed 2.4 GHz/5.8 GHz dual-band monopole antenna with a protruding stub in the ground plane for WLAN and RFID applications," *Progress In Electromagnetics Research*, Vol. 117, 425–434, 2011.
15. Li, B., Z. H. Yan, T. L. Zhang, and C. Wang, "Dual-band antenna with U-shaped open stub for WLAN/WIMAX applications," *Journal of Electromagnetic Waves and Applications*, Vol. 25, Nos. 17–18, 2505–2512, 2011.
16. Li, Z. Q., C. L. Ruan, L. Peng, and X. H. Wu, "Design of a simple multi-band antenna with a parasitic C-shaped strip," *Journal of Electromagnetic Waves and Applications*, Vol. 24, No. 14–15, 1921–1929, 2010.

17. Liu, Z. Y., Y. Z. Yin, L. H. Wen, W. C. Xiao, Y. Wang, and S. L. Zuo, "A Y-shaped tri-band monopole antenna with a parasitic M-strip for PCS and WLAN applications," *Journal of Electromagnetic Waves and Applications*, Vol. 24, Nos. 8–9, 1219–1227, 2010.
18. Lee, S. H. and Y. Sung, "Multiband antenna for wireless USB dongle applications," *IEEE Antennas and Wireless Propagation Letters*, Vol. 10, 25–28, 2011.
19. Liu, S.-X. and Q. Feng, "Compact multi-band loop antennas using CPW-based CRLH quarter-wave type resonators," *Progress In Electromagnetics Research C*, Vol. 28, 47–60, 2012.
20. Chu, Q. X. and L. H. Ye, "Design of compact dual-wideband antenna with assembled monopoles," *IEEE Transactions on Antennas and Propagation*, Vol. 58, 4063–4066, 2010.
21. Yang, K., H. Wang, Z. Lei, Y. Xie, and H. Lai, "CPW-fed slot antenna with triangular SRR terminated feedline for WLAN/WiMAX applications, *Electronics Letters*, Vol. 47, 685–686, 2011.
22. Hu, W., Y. Z. Yin, P. Fei, and X. Yang, "Compact tri-band square slot antenna with symmetrical L-strips for WLAN/WiMAX applications," *IEEE Antennas and Wireless Propagation Letters*, Vol. 10, 462–465, 2011.
23. Lin, C. C., E. Z. Yu, and C. Y. Huang, "Dual-band rhombus slot antenna fed by CPW for WLAN applications," *IEEE Antennas and Wireless Propagation Letters*, Vol. 11, 2012.